Mathematical Model for the Formation of Thin-Film Composite Membranes by Interfacial Polymerization: Porous and Dense Films

J. Ji,[†,‡] J. M. Dickson,[*,§] R. F. Childs,[†] and B. E. McCarry[†]

Departments of Chemistry and Chemical Engineering, McMaster University, Hamilton, Ontario, Canada, L8S 4L7

Received August 12, 1999

ABSTRACT: A general model for the formation of thin-film composite membranes, that considers both diffusion- and reaction-controlled interfacial polymerization, under non-steady-state conditions, has been developed. Special models for either diffusion-controlled or reaction-controlled interfacial polymerization with steady- and non-steady-state conditions have been obtained by simplification; these agree with similar models, where available, in the literature. The porosity of the thin film is dependent on the amount of water that diffuses with the aqueous monomer into the formed film. The analytical solution for the model is consistent with the effect of diamine concentration and successfully predicts it for a polysulfonamide composite membrane fabricated from 1,2-ethanediamine and a disulfonyl chloride. The model allows simulation of various factors that affect thin-film formation, particularly for those factors that are difficult to measure experimentally. This work significantly extends existing theories and provides an important guide for effective control of the thickness of the surface barrier layer of thin-film composite membranes prepared by interfacial polymerization.

I. Introduction

Since Cadotte[1] first prepared thin-film composite membranes by interfacial polymerization, this route has been widely used for membrane fabrication.[2−4] The importance of this type of membrane has led to a considerable amount of work on the key interfacial polymerization step. However, most of these studies have focused on improving membrane performance by optimizing fabrication and operation parameters. Little attention has been paid to the kinetics of the membrane-supported interfacial polymerization process, despite the importance of understanding the system in order to improve membrane performance.

One of the major difficulties in a kinetic examination of membrane-supported interfacial polymerization is the non-steady-state characteristics of the process. The monomer concentration in the support membrane phase, which decreases with polymerization time, is not easy to monitor experimentally.

In contrast, liquid−liquid interfacial polymerization has been well studied. Morgan and co-workers[5−8] have reported on the polycondensation of diacid chlorides with diamines. These studies have shown that the reaction, which takes place in the organic phase close to the interface between aqueous and organic phases, involves an S_N2 (bimolecular nucleophilic substitution) mechanism.[5−9] Kinetic studies on other systems, such as polyester formation, have been recently reported.[10−12]

A model that is based on constant monomer concentrations in the bulk solutions, independent of polymerization time, has been developed by Enkelmann and Wegner[13,14] for the liquid−liquid interfacial polymerization of hexanediamine and 1,8-octanedicarbonyl chloride. Since the interfacial polymerization reaction is fast, and is diffusion-controlled, only diffusion and the competing hydrolysis were considered in the model.[13,14] Pearson and Williams[15] studied the interfacial polymerization of an isocyanate, dispersed as droplets in a continuous diol phase. Both steady-state and non-steady-state models which considered diffusion and reaction rate were developed and solved numerically.

Mikos and Kiparissides[16] have developed, and solved analytically, a model describing skin formation in suspension polymerization of methyl methacrylate in water, assuming a liquid−liquid interfacial polymerization. The Flory−Huggins theory,[17] developed for a polymer solution in equilibrium, was used to describe the composition of the newly formed polymeric film, requiring a numerical solution. Because of the fast rate of interfacial polymerization, the system remained far from the equilibrium; hence it is questionable to apply the Flory−Huggins theory.

Janssen and te Nijenhuis[18−20] have studied the kinetics of encapsulation by the polycondensation of terephthaloyl dichloride with diethylenetriamine at the interface of an oil-in-water emulsion. The diffusion-controlled model developed was in agreement with experimental results for short polymerization times, with membrane thickness increasing with the square root of polymerization time. However, this model incorrectly predicts the membrane thickness when the polymerization time approaches infinity.

No systematic study had been reported dealing with the relationship between the thin-film thickness and the reaction kinetics of membrane-supported interfacial polymerizations under non-steady-state boundary conditions. However, it is important to understand this system, as fabrication conditions affect the barrier layer thickness and hence permeation properties.[21−27]

Recently, we[28,29] reported the fabrication of thin-film composite polysulfonamide membranes fabricated by the interfacial polymerization of an aliphatic diamine with an aromatic disulfonyl chloride; the thickness of the thin-film barrier layer was found to first increase

* To whom correspondence should be addressed.
[†] Department of Chemistry, McMaster University.
[‡] Current address: Koch Membrane Systems Inc., 850 Main St., Wilmington, MA 01887.
[§] Department of Chemical Engineering, McMaster University.

10.1021/ma991377w CCC: $19.00
Published on Web 12/23/1999

Scheme 1

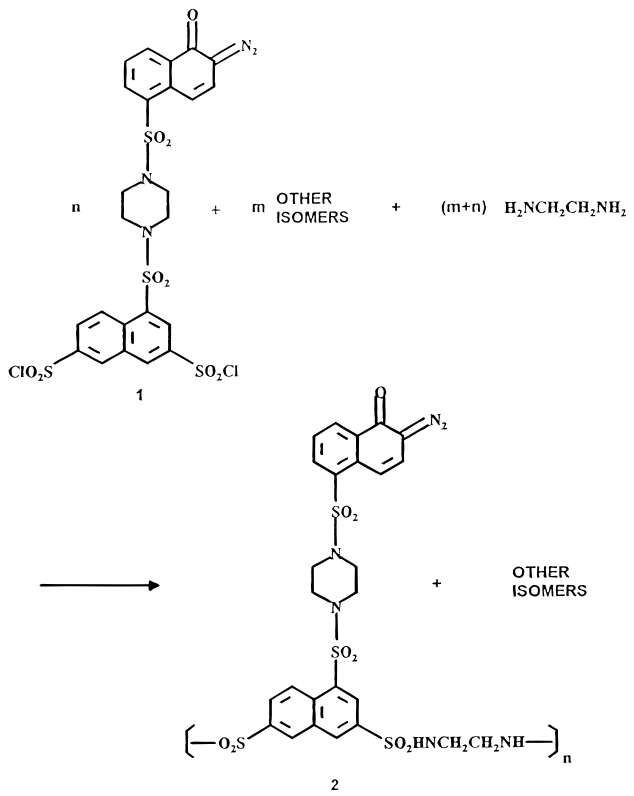

and then level off with polymerization time. In the current work, a general non-steady-state model, which considers both diffusion and reaction, is developed to describe the relationship between the thin-film thickness and the reaction kinetics. The effect of parameters that are difficult to monitor experimentally on thin-film formation, can then be studied by simulation. Subsequently, several special models are derived by simplifying the general model as follows: (1) under non-steady-state boundary conditions, (a) reaction-controlled interfacial polymerization and (b) diffusion-controlled interfacial polymerization; (2) under the conditions of constant monomer concentration in the support membrane phase, (a) both diffusion- and reaction-controlled interfacial polymerization, (b) reaction-controlled interfacial polymerization, and (c) diffusion-controlled interfacial polymerization.

The model can be used to describe the formation of both dense and porous membranes, and the theoretical prediction is compared with experimental results.

To have an experimental system in which growth of the thin film in an interfacial polymerization can be readily studied as a function of time we chose to work with polysulfonamides rather than polyamides. High molecular weight polysulfonamides are known to be produced under interfacial polymerization conditions.[5,6,30,31] The rate of formation of sulfonamide from the reaction of an amine with a sulfonyl chloride is considerably slower than the corresponding reaction with an carboxylic acid chloride to form an amide.[5,6,30,31] This reduced reactivity of the sulfonyl chlorides means that growth of the film is slower and the effects of both reaction and diffusion can be observed.

The system used for comparison purposes in this work was based on the reaction of **1** with 1,2-ethanediamine (see Scheme 1).[28,29] A polysulfone support was first impregnated with an aqueous 1,2-ethanediamine solution and then contacted with a solution of the disulfonyl chloride **1** in a chloroform/carbon tetrachloride mixture. As shown previously, the resulting polysulfonamide, Scheme 1, forms as a porous film on the surface of the support.[28,29]

In the interfacial polymerization of diamines with dicarboxylic acid chlorides reaction occurs in the organic phase close to the interface with the aqueous phase.[5−9] No direct evidence is available on the interfacial formation of polysulfonamides. The organic solvent mixture used here is a very poor solvent for the polysulfonamide **2**, and **1** is not soluble in water. Thus, as with polyamides, the reaction is likely occurring in the organic solvent with precipitation of the polysulfonamide.

There are several kinetic studies reported on the reaction of amines with sulfonyl chlorides. Relevant literature data are summarized in Table 1, with k_{r1} and k_{r2} representing the rate constants of the first and second (if applicable) sulfonamide formation, respectively. In polar solvents, second-order kinetics are typically found.[32−38] However, in nonpolar solvents, the kinetics can be complex with both second- and third-order processes being found. At times it would appear that the reactions may be catalyzed by the presence of a second amine molecule or intramolecularly with a second amine group in a diamine, provided that the intervening chain is of a suitable length.[34]

1,5-Naphthalenedisulfonyl chloride, **3**, was chosen as a close model for the reactions of **1**. Mita and coworkers[34] have reported that the reaction of **3** with primary amines in chloroform is stepwise with k_{r1} greater than k_{r2} by a factor of about ten. Recently, we have developed a direct method, using NMR, to determine these rate constants. For example, in chloroform at 40 °C with 1-butylamine as the primary amine, second-order kinetics were observed, with no statistical difference in k_{r1} (0.053) and k_{r2} (0.057).[36] While chloroform is a good model for the solvent system used in the interfacial polymerization, the presence of water in the reaction zone in the latter case could affect the rates of reaction.

Okamoto et al.[35] studied the reaction of **3** with primary-amino-ended poly(oxyethylenes) in chloroform at 40 °C and found that the reaction rates were independent of chain length from 20 to 20000.

On the basis of this kinetic work, in the model development below, the reaction rate constants of the two sulfonyl chloride groups are assumed to be the same and independent of the degree of polymerization.

II. Theory

A. The General Model: Both Reaction- and Diffusion-Controlled Interfacial Polymerization under Non-Steady-State Boundary Conditions. A general model which considers both diffusion- and reaction-controlled interfacial polymerization under non-steady-state boundary conditions is theoretically developed in this section.

A.1. Model Assumptions. The actual process of membrane-supported interfacial polymerization is complex, and thus assumptions are made to facilitate model formulation. Several authors have made similar simplifying assumptions, explicitly or implicitly, and these are referenced below. The assumptions are:

1. For the interfacial polycondensation of monomer **A** in an aqueous phase with monomer **B** in an organic phase, a small molecule is produced as each condensa-

Table 1. Second-Order Reaction Rate Constants of Amines with Sulfonyl Chlorides

amine or diamine	sulfonyl chloride or disulfonyl chloride	solvent	T, °C	k_{r1}[a]	k_{r2}[a]	ref
aniline	1,4-benzenedisulfonyl chloride	ethyl acetate	25	6.87×10^{-4}	3.42×10^{-4}	32
aniline	1,4-benzenedisulfonyl chloride	nitrobenzene	25	1.51×10^{-3}	6.26×10^{-4}	32
aniline	1,4-benzenedisulfonyl chloride	benzonitrile	25	6.85×10^{-3}	2.49×10^{-3}	32
aniline	1,4-benzenedisulfonyl chloride	acetonitrile	25	1.39×10^{-1}	4.76×10^{-2}	32
aniline	benzenesulfonyl chloride	acetonitrile/water = 9/1	25	4.25×10^{-2}		33
1-butylamine	benzenesulfonyl chloride	acetonitrile/water = 1/1	25	43		33
$H_2N(CH_2)_nNH_2$; n = 6, 8, 10, 12, 14, 16, 18	1,5-naphthalenedisulfonyl chloride	chloroform	40	4.4×10^{-1}	4.8×10^{-2}	34
primary amino ended poly(oxyethylene)	5-dimethylamino-1-naphthalenedisulfonyl chloride	chloroform	40	0.4		35
primary amino ended poly(oxyethylene)	naphthalenesulfonyl chloride ended poly(oxyethylene)	chloroform	40		1.1	35
1-butylamine	1,5-naphthalenedisulfonyl chloride	chloroform	40	0.053	0.057	36

[a] In units of $m^3/(kmol \cdot s)$.

tion reaction occurs which then reacts with monomer **A**; for instance, **A** acts as an acid acceptor with HCl produced. Thus, two molecules of **A** are consumed for each molecule of **B**.

2. The newly formed polymer does not dissolve in either organic or aqueous phases. The density of the thin film is uniform during the reaction.[13,14,18,19]

3. Reaction takes place in a reaction zone of constant thickness, δ, in the organic phase adjacent to the interface.[5,7,8,9]

4. The polymerization reaction has second-order kinetics, with the reaction rate being proportional to the concentrations of both monomers, **A** and **B**.[5,7,8,9]

5. The concentration of **A** in the support-membrane phase is uniform throughout the support membrane.

6. The concentration of **B** is uniform and constant in the organic solution, to the reaction zone, during the polymerization.[13−15]

7. The temperature of the system is uniform.[15]

8. Only monomer **A** is limited by diffusion, from the support-membrane phase to the reaction zone;[13,14] the diffusion coefficient of **A** in the newly formed polymer film is constant.[13,14,18−20]

9. All of **A** arriving at the reaction zone reacts either with monomer **B** to form polymer, with a constant degree of polymerization,[16] or as an acceptor for the condensation product.[5−8]

10. The concentration profile of **A** is linear across the newly formed thin film.[13,14,18,19]

11. Only a fraction, f, of **A** diffuses toward the dense surface to form a barrier layer; the remaining monomer diffuses out through the back of the porous support.

12. The thin film formed by the interfacial polymerization consists of distinct regions of dense polymer and of microvoids.[20,28,29]

13. Monomer **A**, with associated water molecules, diffuses from the support-membrane phase to the reaction zone. The diffusion coefficient of the monomer **A,** with associated water molecules, is assumed to be constant in the newly formed polymeric film.[18−20]

14. Diffusion of **A** is much faster in the voids than in the newly formed polymer.[17,20]

It was shown in our previous work[28,29] that there are microvoids in the newly formed polymer film. A similar microvoid structure was also observed for the capsules formed by interfacial polymerization of terephthaloyl dichloride and diethylenetriamine.[18−20] Janssen and te Nijenhuis[18−20] suggested that the formation of the microvoid structure in the capsule wall was due to the presence of water in the newly formed thin film. The water molecules and diethylenetriamine may diffuse at different rates in the newly formed thin film. However, they assumed that the diethylenetriamine and water diffused together to simplify the model, and this assumption was supported by their experimental results. Therefore, this assumption was adopted and stated as assumption 13 above.

In the 1920s, Evans[39] studied the kinetics of tarnishing and corrosion of metals, such as iron and zinc; a theoretical model considering both diffusion and interfacial reaction was developed to describe the formation of an oxidized layer on the surface of the metals. It was assumed that reactant concentrations in both gaseous and solid phases did not change with reaction time, despite the continuous growth of the oxidized layer. Assumptions 2, 6, 8, and 10 are mathematically similar or adapted from Evans.[39] Assumption 7 was used by Pearson and Williams[15] for the interfacial polymerization of an isocyanate and a diol. Similar assumptions were used by Enkelmann and Wegner[13,14] and by Janssen and te Nijenhuis,[18−20] although many details about how to derive those equations were omitted. As a consequence, they have avoided discussion of the thickness of the reaction zone δ, which is accounted for explicitly in the current work.

A.2. Model Development. Thin film fabrication involves the reaction of an aqueous solution of monomer **A**, such as a diamine, in a support membrane with an organic solvent containing monomer **B**, such as a diacid or disulfonyl chloride.[2,28,29,40,41] Monomer **A**, absorbed by the support membrane, diffuses toward both the top, relatively dense, side[2,28,29,40,41] and the bottom, highly porous, side of the support membrane during the polymerization. A schematic representation of the physical picture for the mathematical model is presented in Figure 1. A full list of symbols is given at the end of the paper. The x coordinate, normal to the support membrane, is fixed at $x = 0$ at the surface of the support membrane. As the film is formed, the polymerization reaction zone moves from the initial location at $x = 0$ to $x = X(t)$ at time t; hence, this is a moving boundary problem. Monomer **A** first partitions into the newly formed polymer and then diffuses to the reaction zone. A typical concentration profile at time t is illustrated in Figure 1.

Given the above assumptions, the following equations can be formulated. At time t, the formation of polymeric thin film due to the second-order reaction is given by

$$\frac{P\rho_P\phi_P}{M_P}\frac{dv_P}{dt} = k_r C(X,t) C_b \delta S \qquad (1)$$

where P is the average degree of polymerization, ρ_P and

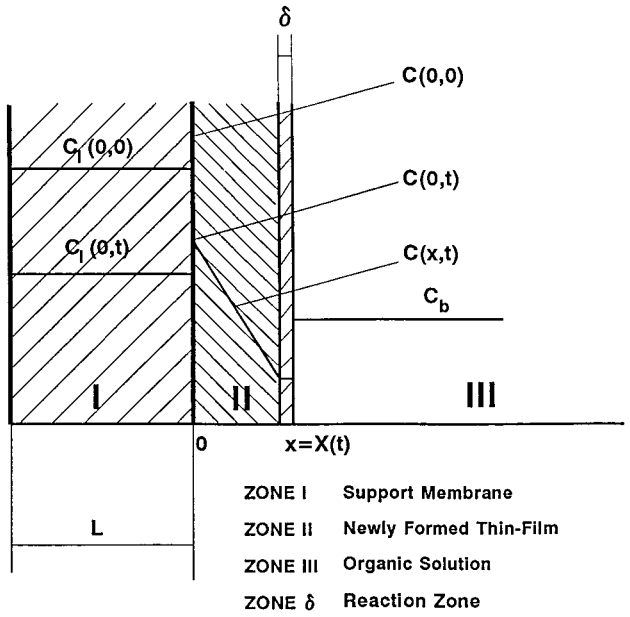

Figure 1. Schematic representation of the model at time t.

ϕ_P are the density and the volume fraction of the polymer of the newly formed polymer film, M_P is the average molecular weight of polymer, dv_P/dt is the volume growth rate of the thin film, k_r is the second-order reaction rate constant, $C(X,t)$ is the concentration of **A** in the reaction zone at time t, C_b is the concentration of **B** in the organic phase, δ is the reaction zone thickness, S is the area, and $dv_P = S\,dX$.

Substitution for dv_P in eq 1 and rearrangement then gives

$$\frac{dX}{dt} = \frac{1}{\phi_P} k_I C(X,t) C_b \tag{2}$$

where dX/dt is the growth rate of the thin-film thickness, which, by assumptions 8, 9, and 12 must be related to the rate of **A** diffusion to the reaction zone, expressed as

$$\frac{P\rho_P\phi_P}{M_P}\frac{dv_P}{dt} = -\frac{S[C(X,t) - C(0,t)]}{\frac{X\phi_V}{D_V} + \frac{X\phi_P}{D_P}} \tag{3}$$

where ϕ_V is the volume fraction of the voids in the thin film ($\phi_V = 1 - \phi_P$) and D_P and D_V are the diffusion coefficients of **A** in the polymer and in the voids, respectively. $C(0,t)$ and $C(X,t)$ are the concentration of **A** at the surface of the support membrane and in the reaction zone, respectively, at time t.

From assumption 14, $D_V \gg D_P$, and after rearrangement, the growth rate of the thin film can be written as

$$\frac{dX}{dt} = \frac{D_M[C(0,t) - C(X,t)]}{X{\phi_P}^2} \tag{4}$$

where D_M is defined as $D_P M_U/\rho_P$.

A material balance on the fraction of **A** that partitions out the top side of the membrane gives

$$\frac{C(0,t)fLS}{K} + \int_0^X C(x,t)\,S\,dx + \frac{2\phi_P XS\rho_P P}{M_P} = \frac{C(0,0)fLS}{K} \tag{5}$$

which describes the un-steady-state concentration of **A**, $C(0,t)$. At time t and in kmol, the first term is the amount of **A** left in the support membrane, the second term is the amount of **A** dissolved in the newly formed film, and the third term is the amount of **A** converted into polymer, which equals the right-hand side, the initial amount of **A** in the support membrane at time zero. Because the condensation reaction produces a small molecule, which in turn reacts with **A**, two molecules of **A** are consumed for each **A** incorporated in the polymer, thus the third term is multiplied by 2.

The concentration profile is linear (assumption 10), and the integral in eq 5 can be solved for the amount of **A** in the thin film as

$$\int_0^X C(x,t)\,S\,dx = \frac{XS[C(0,t) + C(X,t)]}{2} \tag{6}$$

We define the following constants:

$$A_o = \frac{2D_M k_I C_b C(0,0) fL}{{\phi_P}^3} \tag{7}$$

$$B_o = \frac{4KD_M k_I C_b \rho_P}{M_U {\phi_P}^2} \tag{8}$$

$$C_o = \frac{Kk_I C_b}{\phi_P} \tag{9}$$

$$D_o = \frac{2k_I C_b fL}{\phi_P} + \frac{2KD_M}{{\phi_P}^2} \tag{10}$$

$$E_o = \frac{2D_M fL}{{\phi_P}^2} \tag{11}$$

Using eq 3 and assumption 13 (flux of water is proportional to the flux of monomer) gives

$$\phi_P = \frac{M_U\rho_W}{M_U\rho_W + M_W\rho_P\beta} \tag{12}$$

where β is the molar ratio of water to **A** transported (J_W/J_A).

Substitution of eqs 2, 5, and 6 into eq 4 and rearrangement gives the film growth rate as

$$r = \frac{dX}{dt} = \frac{A_o - B_o X}{C_o X^2 + D_o X + E_o} \tag{13}$$

Substitution of eq 13 into eq 2 and rearrangement gives

$$C(X,t) = \frac{\phi_P}{k_I C_b}\frac{A_o - B_o X}{C_o X^2 + D_o X + E_o} \tag{14}$$

Substitution of eq 6 and 14 into eq 5 and rearrangement gives

$$C(0,t) = \frac{1}{\frac{fL}{K} + \frac{X}{2}}\left[\frac{C(0,0)fL}{K} - \frac{2\phi_P X \rho_P}{M_U} - \frac{C(X,t)}{2}X\right] \quad (15)$$

Integration of eq 13, subject to boundary conditions of eqs 14 and 15, gives a relation between t and the thickness, X, as

$$t = -\left(\frac{E_o}{B_o} + \frac{A_o D_o}{B_o^2} + \frac{C_o A_o^2}{B_o^3}\right)\ln\left(1 - \frac{X}{X_{max}}\right) - \frac{C_o}{2B_o}X^2 - \left(\frac{D_o}{B_o} + \frac{C_o A_o}{B_o^2}\right)X \quad (16)$$

When the reaction time, t, approaches infinity, the thin-film thickness, X, approaches a maximum value, X_{max}, and both $C(0,\infty)$ and $C(X,\infty)$ approach zero; X_{max} can be determined by setting eq 13 to zero or, alternatively, dividing eq 7 by eq 8, giving X_{max} as

$$X_{max} = \frac{fM_U C(0,0)L}{2\rho_P K \phi_P} = \frac{A_o}{B_o} \quad (17)$$

Since X_{max} can be obtained experimentally, eq 17 is important because it correlates X_{max} with A_0 and B_0, and it also gives a relationship between f and X_{max}.

The model, given by eq 16 along with eqs 13−15, correctly reduces to the expected values in the time domain. At $t = 0$, the thin-film thickness is zero (eq 16), the maximum growth rate (from eq 13), r_{max}, is proportional to the initial monomer concentration

$$r_{max} = \frac{dX}{dt}\Big|_{t=0}\frac{A_o}{E_o} = \frac{k_I C(0,0) C_b}{\phi_P} \quad (18)$$

and both eqs 14 and 15 correctly reduce to the initial concentration of monomer **A**, $C(0,0)$. As X approaches X_{max}, the right-hand side of eq 16 approaches infinity, the film growth rate correctly approaches zero, from eq 13 as

$$r_{min} = \frac{dX}{dt}\Big|_{t=\infty} = \frac{A_o - B_o X_{max}}{C_o X_{max}^2 + D_o X_{max} + E_o} = 0 \quad (19)$$

and eq 15 and eq 14 give $C(0,\infty) = 0$ and $C(X,\infty) = 0$, respectively.

Thus, the model at various limits is physically reasonable. In summary, eq 16 provides an analytical solution for the formation of thin-film composite membranes.

Note that, for the formation of a dense film ($\phi_P = 1$), eqs 13−16 can be derived independently without assumptions 12−14.

B. Special Models. Several special models can be derived by simplifying the general model.

B.1. Interfacial Polymerization under Non-Steady-State Boundary Conditions. Under non-steady-state boundary conditions, the following special models can be obtained.

B.1.1. Reaction-Controlled Interfacial Polymerization. If the reaction rate of interfacial polymerization is much slower than that of monomer diffusion ($k_I \ll D_M$), the growth rate of the thin film is controlled by the interfacial reaction. In this situation, $C(0,t) = C(X,t)$; therefore, eq 16 reduces to

$$t = -\left(\frac{X_{max}\phi_P}{k_I C_b C(0,0)} + \frac{X_{max} M_U}{2\rho_P k_I C_b}\right)\ln\left(1 - \frac{X}{X_{max}}\right) - \frac{M_U}{2\rho_P k_I C_b}X \quad (20)$$

Equation 20 can also be independently obtained based on the general assumptions discussed previously plus the assumption about the rate-determining step specified in this section.

B.1.2. Diffusion-Controlled Interfacial Polymerization. If the interfacial reaction is much faster than monomer diffusion ($D_M \ll k_I$), then diffusion becomes the rate-determining step. Under this condition, $C(X,t) = 0$, and eq 16 reduces to

$$t = -\left(\frac{X_{max}\phi_P M_U}{4D_M\rho_P} + \frac{X_{max}\phi_P^2}{D_M C(0,0)}\right)X - \frac{\phi_P M_U}{8D_M\rho_P}X^2 - \left(\frac{X_{max}^2\phi_P M_U}{4D_M\rho_P} + \frac{X_{max}^2\phi_P^2}{D_M C(0,0)}\right)\ln\left(1 - \frac{X}{X_{max}}\right) \quad (21)$$

B.2. Interfacial Polymerization under the Condition of Constant Concentration of Monomer A in the Support Membrane Phase. If the amount of **A** converted to polymer plus the amount of **A** dissolved in the newly formed film are much less than what is left in the support membrane phase, then the concentration of **A** in the support membrane is essentially constant; the second and the third terms on the left-hand side of eq 5 are negligible compared to the first term, thus $C(0,t) \approx C(0,0)$. This condition is approximately satisfied in the early stage of the polymerization, even under non-steady-state boundary conditions.

Although the thickness of the thin film formed by interfacial reaction changes with time, this case is often referred to as a steady-state model in the literature.[39]

B.2.1. Reaction- and Diffusion-Controlled Interfacial Polymerization. Assuming that both reaction rate and monomer diffusion are rate-controlling steps, eq 2 still holds and eq 4 is replaced by

$$\frac{dX}{dt} = \frac{D_M[C(0,0) - C(X,t)]}{X\phi_P^2} \quad (22)$$

Substitution of eq 2 into eq 22 and rearrangement gives the thin film growth rate as

$$\frac{dX}{dt} = \frac{D_M k_I C(0,0) C_b}{k_I C_b \phi_P^2 X + D_M \phi_P} \quad (23)$$

Integration of eq 23 gives

$$t = \frac{\phi_P^2 X^2}{2D_M C(0,0)} + \frac{\phi_P X}{k_I C_b C(0,0)} \quad (24)$$

Evans[39] derived equations similar to eqs 2 and 22 based on a consideration of both diffusion and interfacial reaction, but did not solve these equations simultaneously, i.e., no equation similar to eq 24 was obtained. Instead, the equations were solved for two special cases: (1) the diffusion was a rate-controlling step, and (2) the reaction was a rate-controlling step.[39]

B.2.2. Reaction-Controlled Interfacial Polymerization. If the rate of diffusion is much larger than that

of reaction, i.e., $D_M \gg k_I$, then the first term on the right-hand side of eq 24 is negligible compared to the second; thus, eq 24 reduces and rearranges to

$$X = \frac{1}{\phi_P} k_I C(0,0) C_b t \tag{25}$$

which is mathematically the same as that obtained by Evans.[39]

B.2.3. Diffusion-Controlled Interfacial Polymerization. If the reaction rate constant is much larger than that of diffusion, i.e., $k_I \gg D_M$, then the second term on the right-hand side of eq 24 is negligible compared to the first; thus, eq 24 reduces and rearranges to

$$X = \frac{1}{\phi_P} \sqrt{2 D_M C(0,0) t} \tag{26}$$

which is again mathematically the same as that obtained by Evans[39] and is essentially the same as that reported by Janssen and te Nijenhuis.[18−20]

III. Experimental Section

Full details of membrane fabrication and characterization are given elsewhere.[28,29] Briefly, 1,2-ethanediamine, chloroform, dichloromethane, and carbon tetrachloride were reagent grade and used without further purification (Aldrich Chemicals Inc.). A disulfonyl chloride-containing monomer, **1**, which is an isomeric mixture of 1-[4-(2-diazo-1-oxo-1,2-dihydro-5-sulfonyl)naphthalenyl-1-piperazinyl]sulfonyl-3,6-naphthalenedisulfonyl chloride, 3-[4-(2-diazo-1-oxo-1,2-dihydro-5-sulfonyl)-naphthalenyl-1-piperazinyl]sulfonyl-1,6-naphthalenedisulfonyl chloride, and 6-[4-(2-diazo-1-oxo-1,2-dihydro-5-sulfonyl)-naphthalenyl-1-piperazinyl]sulfonyl-1,3-naphthalenedisulfonyl chloride, was prepared as described previously.[28,29]

The concentration of aqueous 1,2-ethanediamine in the support membrane was measured by titration with 0.1 N hydrochloric acid. The thickness of the thin-film layer was measured using a scanning electron microscope (JEOL 1200 EX II, 80 kV, 20K× magnification). The area occupied by the pores in the cross section of the thin-film layer was measured using a Sigma Scan System.[42] The porosity of the thin film was obtained from the ratio of the area occupied by pores to the total area of the cross section of the membrane surface layer.[18−20] At least 17 and an average of more than 30 measurements were made in different locations to determine the mean and standard deviation of thin-film thickness. For the porosity, 17 measurements were conducted, with no clear trend in porosity with membrane thickness; the mean and standard deviations were 0.35 and 0.1, respectively.

IV. Results and Discussion

A. Comparison of Theoretical Prediction with Experimental Results. The general model developed above needs to be compared to the experimental data. For this purpose, 1,2-ethanediamine, the disulfonyl chloride **1**, and HCl are the molecules corresponding to monomer **A**, monomer **B**, and molecule **Z**, respectively. The partition coefficient of diamine between the support membrane and the newly formed thin film, K, is reasonably approximated as 1.0. In the parameter estimation routine, for every guess of X_{max}, f can be calculated from eq 17; once f is determined it can be assumed to be constant. Thus, all of the variables in the model are known and are listed in Table 2, except for three parameters: the diffusion coefficient of 1,2-ethanediamine in the newly formed thin film, D_P, the apparent reaction rate constant, k, and the maximum film thickness, X_{max}.

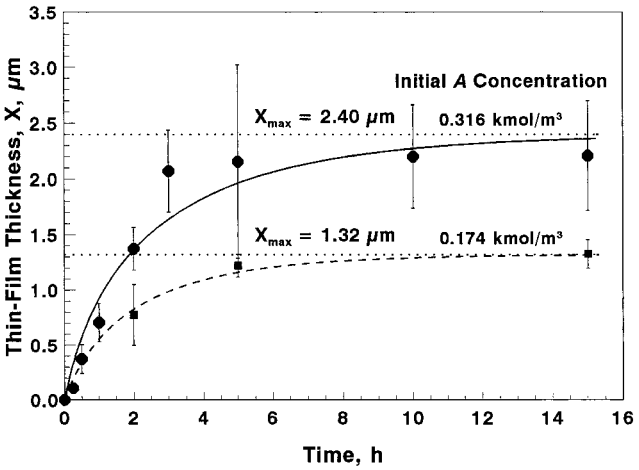

Figure 2. Comparison of the theoretical model with experimental data (points). Parameters are determined at the higher initial **A** concentration and used to predict the curve at the lower initial **A** concentration. The remaining parameters are from Tables 2 and 3. $k = 2.48 \times 10^{-6}$ m^4/(kmol·s); $D_P = 1.64 \times 10^{-15}$ m^2/s.

Table 2. Variables Used in Fitting the Model to Experimental Data

$C(0,0) = 0.316$ kmol/m^3
$C_b = 6.89 \times 10^{-4}$ kmol/m^3
$D_P = 1.64 \times 10^{-15}$ m^2/s
$K = 1.0$ (dimensionless)
$L = 2.05 \times 10^{-4}$ m
$M_A = 60.1$ kg/kmol
$M_B = 705.6$ kg/kmol
$M_Z = 36.45$ kg/kmol
$\rho_P = 1300$ kg/m^3
$\phi_P = 0.65$ (dimensionless)

The real second-order reaction rate constant, k_r, cannot be directly estimated from the current work. However, the order of magnitude of k_r can be calculated from the apparent reaction rate constant, k, and the approximate value of the reaction zone thickness, δ.

A.1. Fitting the Model to Experimental Data. The experimental data are compared to the model as film thickness vs polymerization time in Figure 2. The points and error bars in Figure 2 are means and ±1 standard deviations of the measured average thickness. The model was compared with these experimental results, using a modified Marquardt nonlinear parameter estimation routine, UWHAUS.[43] Initial attempts to fit all three of the above parameters were unsuccessful; the D_P and k values were highly cross correlated, and the program could not converge to reasonable estimates. Therefore, various values of D_P were selected and UWHAUS used to determine k and X_{max}.

Systematically varying D_P from 4.16×10^{-16} to 1.64×10^{-9} m^2/s, while keeping the other parameters fixed, and fitting the values of k and X_{max}, produced no significant change in the curve compared to the curve (at $C(0,0) = 0.316$ kmol/m^3) in Figure 2. Values of D_P lower than 4.16×10^{-16} would not converge to a solution. Fixing on a reasonable, but arbitrary, value of $D_P = 1.64 \times 10^{-15}$ m^2/s gave the actual curve in Figure 2 and the parameter estimates in Table 3. The scatter in the data and the rather large standard deviations on some of the measurements resulted in a rather large 95% confidence interval for k. However, the maximum thickness was determined within about ±15%. The cross correlation coefficient between k and X_{max} is small, indicating that these two parameters are independent estimates.

Table 3. Results of Data Fitting with 95% Confidence Intervals

apparent reaction rate constant, k	$(2.48 \pm 1.41) \times 10^{-6}$ m^4/(kmol·s)
maximum thin-film thickness, X_{max}	$(2.40 \pm 0.40) \times 10^{-6}$ m
correlation coefficient between k and X_{max}	−0.46
number of degrees of freedom	7
fraction of **A** diffusing from top of support, f, calculated from X_{max} and eq 17	0.0904

To further evaluate the model, the above parameters determined at the higher diamine concentration where then used to predict the film thickness at a lower diamine concentration ($C(0,0) = 0.174$ kmol/m^3). The result is presented as the dashed curve in Figure 2. As can be seen, the fit of this true prediction to actual data is excellent. As a further test, the lower diamine concentration data were fitted to the model, and used to predict the results at the higher diamine concentration. There was practically no difference in the shape of the curves or the parameter estimates, indicating that the data and model are consistent. The model is therefore able not only to describe the maximum film thickness but also to predict the effect of diamine concentration. Thus, the parameters listed in Tables 2 and 3 are reasonable.

The diffusion coefficient of a solute in a polymer can range from about 1.0×10^{-10} to 1.0×10^{-20} m^2/s, depending on the physicochemical nature of solute and polymer.[44] The diffusion coefficient of 1,2-ethanediamine in the thin film selected in the above data fitting is indeed within the range reported in the literature and close to the diffusion coefficient of 1,6-hexanediamine in polyamide, 8.0×10^{-14} m^2/s.[45]

Estimation of the real second-order reaction rate constant, k_r, is difficult, because the exact reaction zone thickness, δ, is not known ($k_r = k/\delta$). McRitchie[9,46] has discussed δ qualitatively and concludes that orientation and solvation in the reaction zone affect the thickness. McRitchie's work, combined with discussions by Morgan,[5−8] leads to an approximate range of δ values of about 2−100 nm, which gives $k_r = 1240-24.8$ m^3/(kmol·s), respectively. This range of k_r values is consistent with the reaction rate constant (43.0 m^3/(kmol·s)) for benzenesulfonyl chloride with 1-butylamine in acetonitrile−water,[33] but is 2−3 orders of magnitude larger than the reaction rate constant (0.44) for 1,5-naphthalenedisulfonyl chloride with the alkylamines.[34]

As discussed above, the second-order reaction rate constant is higher in more polar solvents. In this work, the interfacial polymerization takes place at the interface between an aqueous solution and an organic solution of chloroform and carbon tetrachloride. Then, in this relatively polar solvent, the reaction rate constant should be large. In addition, the relatively high value of k_r is due in part to the following: the large error associated with the parameter estimation, the unknown reaction zone thickness, the estimate of the diffusion coefficient, and the other assumptions made in the model.

The above results and discussion suggest that the order of magnitude of the estimated diffusion coefficient, D_P, and the reaction rate constant, k_r, are at least reasonable. However, without independent estimates of D_P or k_r and the reaction zone thickness, δ, these parameters cannot be known with certainty. On the other hand, the maximum film thickness is determined accurately by fitting data to the model.

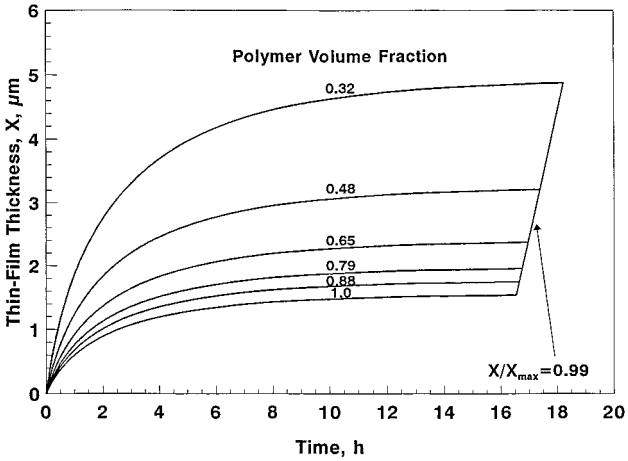

Figure 3. Effect of polymerization time and polymer volume fraction on the thin-film thickness. The curves are produced using eq 16 and the parameters in Tables 2 and 3.

Table 4. Relationship of Polymer Volume Fraction, ϕ_P, to Molar Ratio, β, of Water to 1,2-Ethanediamine Diffused Together in the Thin Film

β	0	4	8	16	32	64
ϕ_P	1.0	0.88	0.79	0.65	0.48	0.32

B. Effect of Water Diffusion on the Thickness of the Thin Film. The model developed in this work allows the formation of a porous film by considering the simultaneous water and diamine diffusion. The relationship between the polymer volume fraction, ϕ_P, in the thin film and the molar ratio of water to diamine flux, β, is given by eq 12; for the current system this relationship is presented in Table 4.

The model presented here assumes implicitly that the porosity of the formed film is uniform. For the actual membranes fabricated a gradation in pore size was noted in the SEM cross sections;[28,29] similar results for a different system were reported elsewhere.[18−20] As well, for these membranes to exhibit reverse osmosis behavior, it is expected that the initial film formed is rather dense, and this is followed by the slower formation of a more porous layer on top of the initial film formed. Thus, in applying the model to these data we are implicitly assuming that the porosity and diamine diffusivity in the formed film are effectively average values.

From Table 4, as the amount of water transported increases, corresponding to increasing β, the polymer volume fraction, ϕ_P, decreases, as expected. If no water molecules are transported with the diamine monomer, then the polymer fraction in the thin film is 1.0; this indicates that a dense membrane is formed.

A typical effect of the polymer volume fraction on the thickness of the thin film is displayed in Figure 3. At a given polymerization time, the thin-film thickness increases with deceasing volume fraction of the polymer in the thin film. These simulations indicate the importance of water transport from the support membrane into the forming thin film on the porosity and thickness of the surface layer of thin-film composite membranes.

C. Kinetic Behavior of Thin-Film Formation by Interfacial Polymerization. Having established the model and approximated a set of parameters, then the effects of different factors on the kinetics of the interfacial polymerization and on the formation of the thin film can be studied. In particular, those parameters which are difficult to measure experimentally are of

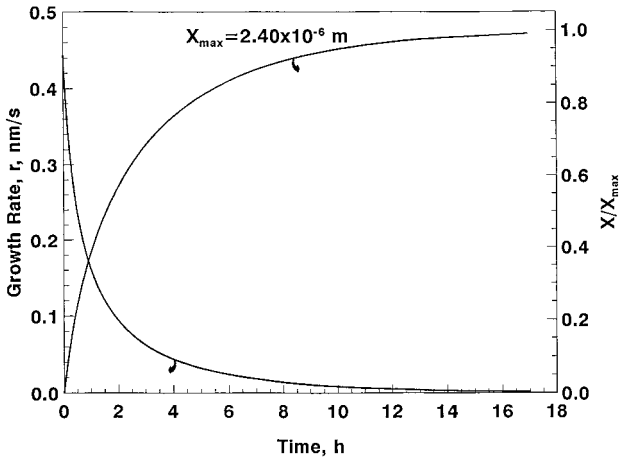

Figure 4. Effect of polymerization time on the growth rate and the reduced thickness of the thin film, with different polymer volume fractions. The curves are produced using eqs 13, 16, and 17 and the parameters in Tables 2 and 3.

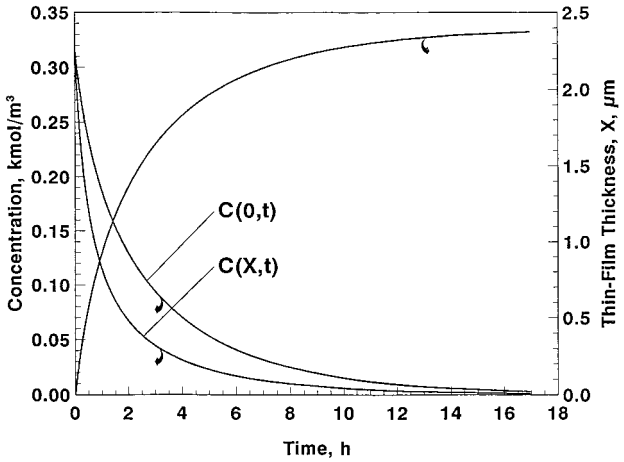

Figure 5. Effect of polymerization time on the concentrations of 1,2-ethanediamine at the surface of the support membrane and in the reaction zone and the thin-film thickness, with different polymer volume fractions. The curves are produced using eqs 14, 15, and 16 and the parameters in Tables 2 and 3.

interest. The diamine diffusion coefficient, the apparent reaction rate constant, and the parameters in Tables 2 and 3, except where noted otherwise, are used in the following simulations.

The reduced thickness, X/X_{max}, is equivalent to the diamine reaction conversion. The effect of polymerization time on thin-film growth rate and on the reduced thickness, as a function of polymer volume fraction, is illustrated in Figure 4. The thin-film growth rate, the reduced thickness, and the maximum thickness are calculated by eqs 13, 16, and 17, respectively. The growth rate decreases rapidly with polymerization time for up to about 2 h and then levels off, approaching zero. The reduced thickness increases with time, opposite to the growth rate, as expected. The initial thin-film growth rate is inversely proportional to the polymer volume fraction, by eq 18.

The maximum thin-film thickness is similarly inversely proportional to the polymer volume fraction, by eq 17. However, the reduced thickness is effectively independent of the polymer volume fraction, as the four curves in Figure 4 at different volume fractions are nearly superimposed. Thus, increased porosity of the thin-film increases both the growth rate and the thin-film thickness at any reaction time.

The effect of polymerization time on thin-film thickness, on the concentrations of 1,2-ethanediamine at the surface of the support membrane, $C(0,t)$, and in the reaction zone, $C(X,t)$, concentration, are simulated from the model (using eqs 14 to 16 and the parameters in Tables 2 and 3) and depicted in Figure 5. The effect of increasing polymer volume fraction is to decrease the thin-film thickness, as discussed above.

The concentrations $C(0,t)$ and $C(X,t)$ rapidly decrease during the polymerization for up to 2 h and then finally approach zero. The concentration profiles with time are independent of polymer volume fraction. The driving force for diffusion, $(C(0,t) - C(X,t))$, is initially small, as the thin film starts to grow. As time proceeds, the driving force increases, indicating the importance of diffusion on the film growth rate, and finally decreases as the diamine is consumed and the polymerization becomes controlled by the reaction kinetics. Thus, for this real case of polysulfonamide thin-film composite membrane formation, both diffusion and reaction rates are important.

V. Conclusion

A theoretical model describing both diffusion- and reaction-controlled interfacial polymerization of microporous thin-film composite membranes under non-steady-state conditions has been developed. This general model could be reduced to the following special models under the following given conditions: (1) non-steady-state boundary conditions, (a) reaction-controlled interfacial polymerization and (b) diffusion-controlled interfacial polymerization; (2) constant monomer concentration in the support membrane phase, (a) diffusion- and reaction-controlled interfacial polymerization, (b) reaction-controlled interfacial polymerization, and (c) diffusion-controlled interfacial polymerization.

The analytical solutions to cases 2b and 2c agreed with those published earlier. All the models developed are simple, have easy to use analytical solutions, have clear physical meaning, and predict results that would be expected for interfacial polymerization. The model correctly reduces to the dense film case when water diffusion into the forming film is zero. The model is consistent with experimental results for the formation of polysulfonamide thin-film composite membranes from 1,2-ethanediamine and a disulfonyl chloride. Because of the interdependence of the diffusivity and reaction rate constant in the model, these parameters cannot be determined exactly. However, values deduced from the data fitting are reasonably consistent with those expected from the literature.

Model simulations allow the calculation of various factors, including the amount of water that transfers with the diamine into the thin-film and the effect of diamine concentration, on the porosity, growth rate, and thickness of the thin film. Simulation trends are as expected and the prediction of the effect of diamine concentration is consistent with experimental data. Increasing the polymer volume fraction acts to reduce both the thin-film growth rate and maximum thickness. The concentration profiles and the reduced thickness, as a function of time, are independent of the polymer volume fraction.

This work has significantly extended the existing theories of thin-film formation by interfacial polymerization. The model developed in this work provides a

tool for studying and understanding of the kinetics of interfacial polymerization and provides an important guide for effective control of the thickness of the surface barrier layer of thin-film composite membrane prepared by interfacial polymerization.

Although the models discussed above are developed for polymeric membrane-supported interfacial polymerization, they are mathematically suitable for any kind of interfacial polymerization and for reactions of small molecules which satisfy the assumptions used to develop the models.

Acknowledgment. The authors would like to thank the financial support of the Natural Sciences and Engineering Research Council Canada (NSERC), 3M Canada Inc., and the University Research Incentive Fund (URIF). The authors would also like to thank Dr. M. G. Liu for help with computer programming.

List of Symbols

A_0	constant defined in eq 7, $m^7/(kmol \cdot s^2)$
B_0	constant defined in eq 8, $m^6/(kmol \cdot s^2)$
C_0	constant defined in eq 9, $m^4/(kmol \cdot s)$
$C(x,t)$	concentration of monomer **A** in the thin film at position x and time t, as shown in Figure 1, $kmol/m^3$
$C_I(0,t)$	concentration of monomer **A** in the support-membrane phase at time t, as shown in Figure 1, $kmol/m^3$
C_b	concentration of monomer **B** in the organic phase, as shown in Figure 1, $kmol/m^3$
D_i	diffusion coefficient of monomer **A** at i in the thin film, m^2/s
D_0	constant defined in eq 10, $m^5/(kmol \cdot s)$
D_M	effective diffusion coefficient, $D_P M_U/\rho_P$, in eq 4, $m^5/(kmol \cdot s)$
E_0	constant defined in eq 11, $m^6/(kmol \cdot s)$
f	fraction of **A** that diffuses out the top of the support membrane, $0 < f < 1$
K	partition coefficient of monomer **A** between the support and the thin-film phases
k	apparent reaction rate constant, $k_r\delta$, $m^4/(kmol \cdot s)$
k_I	constant in eq 2, $k_r\delta M_U/\rho_P$, $m^7/(kmol^2 \cdot s)$
k_r	second-order reaction rate constant, $m^3/(kmol \cdot s)$
L	thickness of the support membrane, as shown in Figure 1, m
M_i	molecular weight of component i, kg/kmol
M_P	average molecular weight of the polymer, PM_U, kg/kmol
M_U	molecular weight of the repeat unit, $M_A + M_B - 2M_Z$, kg/kmol
P	average degree of polymerization
r	growth rate of the thin film, m/s
S	membrane area, m^2
t	polymerization time, s
v_P	volume of the thin film, zone II in Figure 1, m^3
x	coordinate normal to the membrane surface, m
X	thickness of the thin film, as shown in Figure 1, m

Greek Letters

β	molar ratio of water to monomer A transported together dy diffusion
δ	thickness of the reaction zone as shown Figure 1, m
ρ_i	density of i, kg/m^3
ϕ_i	volume fraction i in the thin film

Subscripts

A	monomer **A**
B	monomer **B**
min	minimum value
max	maximum value
P	average polymer
U	repeat unit
V	microvoids
W	water
Z	a small molecule formed from each condensation reaction

References and Notes

(1) Cadotte, J. E. U.S. Patent 4,039,440, 1977.
(2) Petersen, R. J. *J. Membr. Sci.* **1993**, *83*, 81−150.
(3) Rozelle, L. T.; Cadotte, J. E.; Kobian, K. E.; Kopp, C. V. Jr. In *Reverse Osmosis and Synthetic Membranes*; Sourirajan, S., Ed.; National Research Council Canada: Ottawa, 1977; p 249.
(4) Petersen, R. J.; Cadotte, J. E. In *Handbook of Industrial Membrane Technology*; Porter, M. C., Ed.; Noyes Publications: Park Ridge, NJ, 1990; p 307.
(5) Morgan, P. W. *Condensation Polymers: By Interfacial and Solution Methods*; Interscience Publishers: John Wiley & Sons: New York, 1965.
(6) Morgan, P. W. In *Encyclopedia of Polymer Science and Engineering*; Mark, H. F., Bikales, N. M., Overberger, C. G., Menges, G., Kroschwitz, J. I., Eds.; John Wiley & Sons: New York, 1985; Vol. 8, p 221.
(7) Morgan, P. W.; Kwolek, S. L. *J. Polym. Sci.* **1959**, *40*, 299−327.
(8) Morgan, P. W. *J. Polym. Sci., Polym. Symp.* **1985**, *72*, 27−37.
(9) MacRitchie, F. In *Interfacial Synthesis Vol. I, Fundamentals*; Millich, F., Carraher, C. E., Jr., Eds.; Marcel Dekker: New York, 1977;. p 103.
(10) Tsai, H. B.; Lee, Y. D. *J. Polym. Sci., Part A: Polym. Chem.* **1987**, *25*, 1505−1515.
(11) Tsai, H. B.; Lee, Y. D. *J. Polym. Sci., Part A: Polym. Chem.* **1987**, *25*, 2195−2206.
(12) Kosky, P. G.; Boden, E. P. *J. Polym. Sci., Part A: Polym. Chem.* **1990**, *28*, 1507−1518.
(13) Enkelmann, V.; Wegner, G. *Makromol. Chem.* **1972**, *157*, 303−306.
(14) Enkelmann, V.; Wegner, G. *Appl. Polym. Symp.* **1975**, *26*, 365−372.
(15) Pearson, R. G.; Williams, E. L. *J. Polym. Sci., Polym. Chem.* **1985**, *23*, 9−18.
(16) Mikos, A. G.; Kiparissides, C. *J. Membr. Sci.* **1991**, *59*, 205−217.
(17) Flory, P. J. *Principles of Polymer Chemistry*; Cornell University Press: Ithaca, NY, 1953.
(18) Janssen, L. J. J. M.; te Nijenhuis, K. *J. Membr. Sci.* **1992**, *65*, 59−68.
(19) Janssen, L. J. J. M.; te Nijenhuis, K. *J. Membr. Sci.* **1992**, *65*, 69−75.
(20) Janssen, L. J. J. M.; A. Boersma, te Nijenhuis, K. *J. Membr. Sci.* **1993**, *79*, 11−26.
(21) Kimura, S.; Sourirajan, S. *AIChE J.* **1967**, *13*, 497−503.
(22) Lonsdale, H. K.; Merten, U.; Riley, R. L. *J. Appl. Polym. Sci.* **1965**, *9*, 1341−1362.
(23) Soltanieh, M.; Gill, W. N. *Chem. Eng. Commun.* **1981**, *12*, 279−363.
(24) Pusch, W. *Desalination* **1986**, *59*, 105−198.
(25) Dickson, J. M. In *Reverse Osmosis Technology, Application for High-Purity−Water Production*; Parekh, B. S., Ed.; Marcel Dekker: New York, 1988; pp 1−50.
(26) Mehdizadeh, H.; Dickson, J. M. *J. Membr. Sci.* **1989**, *42*, 119−145.
(27) Mason, E. A.; Lonsdale, H. K. *J. Membr. Sci.* **1990**, *51*, 1−81.
(28) Ji, J.; Trushinski, B. J.; Childs, R. F.; Dickson, J. M.; McCarry, B. E. *J. Appl. Polym. Sci.* **1997**, *64*, 2381−2398.
(29) Ji, J. Ph.D. Thesis, McMaster University, Hamilton, Ontario, Canada, 1996.

(30) Sundet, S. A.; Murphey, W. A.; Speck, S. B. *J. Polym. Sci.* **1959**, *40*, 389−397.
(31) Evers, R. C.; Ehlers, G. F. L. *J. Polym. Sci., Part A-1* **1967**, *5*, 1797−1801.
(32) Kuritsyn, L. V.; Kuritsyna, V. M. *J. Org. Chem. USSR* **1972**, *8*, 103−104.
(33) Ciuffarin, E.; Senatore, L.; Isola, M. *J. Chem. Soc., Perkin Trans. 2* **1972**, 468−471.
(34) Mita, I.; Toyoshima, K.; Okamoto, A. *Eur. Polym. J.* **1983**, *19*, 657−660.
(35) Okamoto, A.; Toyoshima, K.; Mita, I. *Eur. Polym. J.* **1983**, *19*, 341−346.
(36) Schmidt, K.; Childs, R. F.; Dickson, J. M. Unpublished data, 1997.
(37) Litvinenko, L. M.; Maleeva, N. T.; Savelova, V. A.; Kovach, T. D. *J. Gen. Chem. USSR* **1971**, *41*, 2648−2650.
(38) Arcoria, A.; Librando, V.; Maccarone, E.; Musumarra, G.; Tomaselli, G. A. *Tetrahedron* **1977**, *33*, 105−111.
(39) Evans, U. R. *Trans. Am. Electrochem. Soc.* **1925**, *46*, 247−282.
(40) Cadotte, J. E.; King, R. S.; Majerle, R. J.; Petersen, R. J. *J. Macromol. Sci. Chem.* **1981**, *A15*, 727−755.
(41) Trushinski, B. J.; Dickson, J. M.; Childs, R. F.; McCarry, B. E. *J. Appl. Polym. Sci.* **1993**, *48*, 187−198.
(42) Parker, D. R.; Norby, J.; Bennington, J. *Sigma Scan Scientific Measurement System*; Jandel Scientific: Corte Madera, CA, 1988.
(43) Meeter, D. A. *Nonlinear Least Squares (UWHAUS)*; University of Wisconsin Computing Center: Madisom, WI, 1965.
(44) Crank, J., Park, G. S., Eds., *Diffusion in Polymers*; Academic Press: New York, 1968.
(45) Enkelmann, V.; Wegner, G. *J. Appl. Polym. Sci.* **1977**, *21*, 997−1007.
(46) MacRitchie, F. *Trans. Faraday Soc.* **1969**, *65*, 2503−2507.

MA991377W